



HAL
open science

Experimental assessment of ammonia adiabatic absorption into ammonia-lithium nitrate solution using a flat fan nozzle.

A. Zacarías, M. Venegas, R. Ventas, A. Lecuona

► **To cite this version:**

A. Zacarías, M. Venegas, R. Ventas, A. Lecuona. Experimental assessment of ammonia adiabatic absorption into ammonia-lithium nitrate solution using a flat fan nozzle.. *Applied Thermal Engineering*, 2011, 31 (16), pp.3569. 10.1016/j.applthermaleng.2011.07.019 . hal-00789880

HAL Id: hal-00789880

<https://hal.science/hal-00789880>

Submitted on 19 Feb 2013

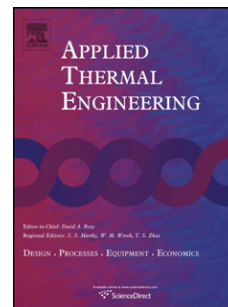
HAL is a multi-disciplinary open access archive for the deposit and dissemination of scientific research documents, whether they are published or not. The documents may come from teaching and research institutions in France or abroad, or from public or private research centers.

L'archive ouverte pluridisciplinaire **HAL**, est destinée au dépôt et à la diffusion de documents scientifiques de niveau recherche, publiés ou non, émanant des établissements d'enseignement et de recherche français ou étrangers, des laboratoires publics ou privés.

Accepted Manuscript

Title: Experimental assessment of ammonia adiabatic absorption into ammonia-lithium nitrate solution using a flat fan nozzle.

Authors: A. Zacarías, M. Venegas, R. Ventas, A. Lecuona



PII: S1359-4311(11)00376-0

DOI: [10.1016/j.applthermaleng.2011.07.019](https://doi.org/10.1016/j.applthermaleng.2011.07.019)

Reference: ATE 3646

To appear in: *Applied Thermal Engineering*

Received Date: 15 December 2010

Revised Date: 6 June 2011

Accepted Date: 10 July 2011

Please cite this article as: A. Zacarías, M. Venegas, R. Ventas, A. Lecuona. Experimental assessment of ammonia adiabatic absorption into ammonia-lithium nitrate solution using a flat fan nozzle., *Applied Thermal Engineering* (2011), doi: 10.1016/j.applthermaleng.2011.07.019

This is a PDF file of an unedited manuscript that has been accepted for publication. As a service to our customers we are providing this early version of the manuscript. The manuscript will undergo copyediting, typesetting, and review of the resulting proof before it is published in its final form. Please note that during the production process errors may be discovered which could affect the content, and all legal disclaimers that apply to the journal pertain.

Experimental assessment of ammonia adiabatic absorption into ammonia-lithium nitrate solution using a flat fan nozzle.

A. Zacarías^a, M. Venegas^{b,*}, R. Ventas^b, A. Lecuona^b

^a Academia de Térmicas ESIME Azcapotzalco, Instituto Politécnico Nacional, Av. de las Granjas 682, Col. Santa Catarina, 02550, Distrito Federal, Mexico

^b Departamento de Ingeniería Térmica y de Fluidos, Universidad Carlos III de Madrid, Avda. Universidad 30, 28911 Leganés, Madrid, Spain

Abstract

This paper presents the experimental evaluation of the adiabatic absorption of ammonia vapour into ammonia-lithium nitrate solution using a flat fan nozzle and an upstream single-pass subcooler. Data are representative of the working conditions of adiabatic absorbers in absorption chillers. The nozzle was located at the top of the absorption chamber, separated 205 mm from the bottom surface. The diluted solution mass flow rate was modified between 0.04 - 0.08 kg/s and the solution inlet temperature between 24.5 – 29.7 °C. The influence of these variables on the absorption ratio, mass transfer coefficient, outlet subcooling and approach to equilibrium factor is analysed in the present paper. A linear relation between the inlet subcooling and the absorption ratio is observed. The approach to equilibrium factor for the conditions essayed is always between 0.81 and 0.89. Mass transfer coefficients and correlations for the approach to equilibrium factor and the Sherwood number are obtained. Results are compared with other ones reported in the literature.

Keywords: Ammonia-lithium nitrate solution; adiabatic absorption; atomization; flat fan nozzle.

Nomenclature

* Corresponding author. Tel.: +34 916248465; fax: +34 916249430.
E-mail addresses: mvenegas@ing.uc3m.es (M. Venegas).

a	constant of the linear relation $X = a \cdot T + b$ at a given equilibrium pressure in the Dühring diagram, function of pressure, concentration and temperature (K^{-1})
A	area (m^2)
C_1	constant
C_2	constant
C_3	constant
C_p	specific heat at constant pressure ($kJ\ kg^{-1}\ K^{-1}$)
d_o	nozzle inner diameter (mm)
D	liquid mass diffusivity ($m^2\ s^{-1}$)
f	generic function
F	approach to equilibrium factor
F_c	correction factor for the logarithmic mean temperature difference
G	mass flux $G = \dot{m}/A$ ($kg\ m^{-2}\ s^{-1}$)
h	specific enthalpy ($kJ\ kg^{-1}$)
h_m	mass transfer coefficient ($mm\ s^{-1}$)
k	thermal conductivity ($W\ m^{-1}\ K^{-1}$)
H	vertical distance between port centres (mm)
L	effective thermal length (mm)
L^*	characteristic length of the adiabatic chamber (m)
Le	Lewis number ($Le = \alpha/D$)
\dot{m}	total mass flow rate ($kg\ s^{-1}$)
P	pressure (Pa)
Pr	Prandtl number ($Pr = \mu \cdot C_p/k$)
q	heat flux based on the effective area ($W\ m^{-2}$)
\dot{Q}	thermal power (W)
R_a	absorption ratio ($kg_v\ kg_{ds}^{-1}$)
Re	Reynolds number for heat transfer in the subcooler ($Re = G_{cs} D_h / \mu_{cs}$)
Re_a	Reynolds number for mass transfer in the absorber ($Re_a = 4 \dot{m}_{cs} / \pi \mu_{cs} d_o$)
Sc	solution Schmidt number ($Sc = \mu_{cs} / \rho_{cs} D_{cs}$)
Sh	solution Sherwood number ($Sh = h_m L^* / D_{cs}$)
T	temperature ($^{\circ}C$)
U	global heat transfer coefficient ($W\ m^{-2}\ K^{-1}$)

V	volume (m^3)
X	refrigerant mass fraction (%)

Greek symbols

ΔH	absorption heat (kJ)
ΔT	temperature difference, subcooling ($^{\circ}\text{C}$)
ΔT_{lm}	logarithmic mean temperature difference ($^{\circ}\text{C}$)
ΔX	concentration difference (%)
ΔX_{lm}	logarithmic mean concentration difference (%)
α	thermal diffusivity ($\text{m}^2 \text{s}^{-1}$)
φ	Corrugation angle (degrees)
μ	viscosity (Pa s)
ρ	density (kg m^{-3})
σ	surface tension (N m^{-1})

Subscripts

a	absorber, adiabatic
cs	concentrated solution
ds	diluted solution
exp	experimental
eq	equilibrium
i	inlet
l	laminar
o	outlet
SP	simple phase
sin	singularities
t	turbulent
v	vapour
w	water

Acronyms

DI	density indicator
----	-------------------

EQI	energy and volumetric flow indicator
FPHE	fusion plate heat exchanger
LI	liquid level indicator
MVD	mean volume diameter (μm)
PI	pressure indicator
PIC	pressure control
PID	proportional integral derivative control
ΔPI	pressure drop indicator
QI	volumetric flow rate indicator
QIC	volumetric flow rate control
TI	temperature indicator
TIC	temperature control
WI	wattmeter

1. Introduction

In a cooling machine of the absorption type, the absorption process takes place when the refrigerant vapour coming from the evaporator is absorbed by the concentrated solution arriving from the generator, Herold and Radermacher [1]. This process is exothermic and the heat released should be extracted in order to increase the amount of vapour absorbed. Absorption can take place putting into contact solution and vapour in three different relations of geometrical continuity of phases: solution continuous-vapour continuous, solution continuous-vapour discontinuous and solution discontinuous-vapour continuous. Vapour absorption occurs in all cases through the liquid-vapour interface.

The first one consists in supplying the solution as a continuous liquid sheet over the wall of a specific geometry and the vapour also in a continuous way co-currently or counter-currently with the liquid sheet. This is the conventional absorption method used in contemporary commercial absorption machines using water and salts as working fluids, for this being called falling film absorption. Absorption heat is evacuated through the wall.

The second method is based on injecting vapour bubbles into the solution, Infante Ferreira [2], circulating co-currently or counter-currently throughout a specific channel. Channel walls evacuate the absorption heat.

The third method consists of dispersing the solution inside a chamber filled with refrigerant vapour. There is no way of evacuating the absorption heat in the chamber.

The last method is an alternative to conventional designs of absorbers that has received increasing attention in the last years; among others, Ryan [3], Ryan *et al.* [4], Summerer *et al.* [5], Venegas *et al.* [6,7], Arzoz *et al.* [8], Warnakulasuriya and Worek [9,10], Palacios *et al.* [11,12], Acosta-Iborra *et al.* [13], Gutiérrez [14], Zacarías [15] and Ventas [16]. In this configuration, the heat and mass transfer processes are separated into two different devices: the single-phase solution subcooler and the absorption chamber. In the subcooler, the solution is cooled below the saturation temperature, allowing absorption to only take place in the downstream adiabatic chamber. The absorber is known as adiabatic, because heat is not extracted from the solution at the same time the mass transfer process occurs. The claimed advantages of this technique are a more compact absorber and avoidance of the channelling effect and wetting difficulties of the absorber wall surface, problem that has been discussed by Jeong and Garimella [17] among others. In addition to this, a conventional single-phase heat exchanger can be used for the subcooler.

Different possibilities for dispersing the solution inside the adiabatic chamber are available, depending on the nozzle used: flat fan, hollow cone, fog jet, full cone, etc. In the present work, a flat fan nozzle is used to evaluate experimentally the absorption process, as its form factor is potentially compact. A review of this absorption method is performed below, including analytical, numerical and experimental studies.

1.1. Analytical and numerical studies

Acosta-Iborra *et al.* [13] performed the modelling of the adiabatic absorption of refrigerant vapour by expanding liquid sheets, not including the resulting drops. The authors developed four models of different level of approximation to evaluate and compare the absorption process using the water-lithium bromide ($\text{H}_2\text{O-LiBr}$) and the ammonia-lithium nitrate ($\text{NH}_3\text{-LiNO}_3$) properties. The model equations under simplifying assumptions were solved either analytically or numerically under conditions

representative of adiabatic absorption in refrigeration machines. The authors concluded that, using the same inlet concentration and subcooling, the $\text{NH}_3\text{-LiNO}_3$ solution always allows obtaining higher Sherwood numbers, Sh , and absorption ratios, R_a , than the $\text{H}_2\text{O-LiBr}$ pair.

1.2. Experimental studies

The first experiments reported in the open literature regarding adiabatic absorption into conical sheets and flat-fan sheets were developed by Palacios *et al.* [11,12] respectively. In both cases, the solution forms a continuous sheet in the region near the nozzle and subsequently disintegrates into small drops. The authors used the $\text{H}_2\text{O-LiBr}$ solution to characterize experimentally the absorption of water vapour. In [11], the authors reported that, at a nozzle height above the impact surface of 40 mm, the approach to equilibrium factor F amounted 0.76. F means the fraction of the adiabatic equilibrium mass of vapour absorbed. At heights of 220 mm, F reached about 0.93. In both cases, a solution mass flow rate of 42 kg/h was used. Lower solution flow rates had associated lower values of F . In [12], the authors concluded that the adiabatic absorption using a flat-fan nozzle offers better absorption performance than the conventional diabatic falling film absorbers.

Gutiérrez [14] developed experiments using also the $\text{H}_2\text{O-LiBr}$ solution and the dispersion of the liquid using a flat fan nozzle. The author concluded that this configuration obtains better absorption performance than the arrangement using free falling drops.

Commercial absorption machines mainly use the $\text{H}_2\text{O-LiBr}$ solution for air-conditioning purposes, while the $\text{NH}_3\text{-LiNO}_3$ is a promising solution for refrigeration applications (e.g. Venegas *et al.* [18]). As far as the authors' knowledge, experimental studies regarding the adiabatic absorption of ammonia vapour by $\text{NH}_3\text{-LiNO}_3$ solution using a flat fan nozzle are not available. The present paper offers results of an experimental study in order to evaluate the mass transfer capacity of this adiabatic absorption configuration. Besides that, the performance of the upstream subcooler is also evaluated.

2. Experimental setup

The experimental facility used in the present study is configured as a test rig for absorption machine components. It forms a thermo-chemical compressor, integrating a generator, a single-pass absorber and a heat recovery exchanger as main components (see Fig. 1). Auxiliary components are: the external water heater, the solution subcooler and an ammonia vapour cooler. The solution tank serves only for solution preparation and off-line storage for safety. The vapour separator at the outlet of the generator is a long tube of 21.8 mm inner \varnothing and 1.5 m high. More information about the components of the test rig can be found in Zacarías [15] and Zacarías *et al.* [19].

Type PT100 class A temperature sensors are used at the corresponding inlets and outlets of each heat exchanger. All of the heat exchangers are of the fusion plate type (FPHE) made of stainless steel. The adiabatic chamber also incorporates temperature sensors. Pressure in the low and high pressure zones, and at the inlet of the adiabatic chamber, is measured using absolute transducers. Three Coriolis type flow meters, manufactured by RheonikTM, MicromotionTM and YokogawaTM, allow measuring the mass flow rate and density (except the YokogawaTM one) of the concentrated and diluted solution and of the ammonia vapour respectively. The solution pump is of the volumetric type and a variable frequency driver controls its flow rate. All instruments are calibrated using certified calibrators. Table 1 shows the results of an uncertainty analysis for the measured variables used in the present study. Uncertainty results shown were obtained as follows:

- Temperature and pressure: Calibration curves were obtained. A 95% confidence level was used to determine the uncertainty of the thermoresistances and pressure transducers.
- Mass flow rate and density: Uncertainties were given by the manufacturers.

The facility incorporates a data acquisition system controlled by a computer in addition to individual PID controllers for safety. Data gathered by the flow meters and the temperature and pressure transducers are recorded on the computer every 6 s. After an initial stabilization process, data are recorded and averaged for a period of 10 minutes. The three available main control loops are as follows (see Fig. 1):

1. Temperature of the solution at the outlet of the generator (TIC). This control modifies the effective voltage applied to the water heater resistors.

2. Pressure in the absorber (PIC). This control modifies the aperture of the vapour expansion valve.
3. Diluted solution mass flow rate, measured by the flow meter (QIC). It modifies the speed of the solution pump located at the outlet of the absorber.

The charge of refrigerant and lithium nitrate salt inside the test rig allowed keeping the refrigerant mass fraction at $X = 45.35\%$ along the experimentation, with a standard deviation of 0.086% . No internal storage was devised for solution accumulation, see Fig. 1.

Properties of ammonia and water were taken from Engineering Equation Solver software, EESTM [21], which uses respectively the fundamental equation of state developed by [22] and the thermodynamic property correlation of [23]. Solution properties were calculated using correlations given by Libotean *et al.* [24,25] and Libotean [26].

2.1. Subcooler

In adiabatic absorbers the subcooler is used not only to cool the solution flow coming from the generator, but also the recirculated solution, so that a higher absorption ratio is reached, as shown by Gutiérrez [14]. This makes its capability of removing absorption heat of paramount importance. Ventas *et al.* [20] studied the effect of the amount of recirculation on the performance of an ammonia-lithium nitrate single-effect absorption chiller.

No recirculation of the solution is produced in the present study, i.e. the solution is subcooled only once in the subcooler before entering the adiabatic chamber. This forms the basic process for a recirculating absorber, according to Ventas *et al.* [20]. Fig. 2 shows a geometrical scheme of the FPHE used as solution subcooler. Table 2 gives all the geometrical parameters for the particular model used. After absorption, the diluted solution is pumped to the heat recovery exchanger.

2.2. Adiabatic absorption chamber

The adiabatic absorption chamber, shown in Fig. 3a, is a cylindrical vessel constructed on stainless steel with 40 cm of internal diameter, yielding a total internal volume of 0.0542 m³. The absorber has three ports: inlet of concentrated solution (top), inlet of superheated vapour (lateral) and outlet of diluted solution (bottom). Two transducers are used to measure the concentrated solution pressure at the inlet of the absorber and the internal pressure of the chamber. In the internal upper zone of the chamber, one horizontal rail with 3 ports of ¼" diameter is suspended from a vertical pipe of variable length, selected according to the nozzle height to be experimented. The nozzles are connected to one or several of these ports. The absorber is equipped with peepholes in the lateral ends to allow visualizing the atomization process.

Data for the two identical flat fan nozzles used in the present study are shown in Table 3 for nominal differential pressures of 150 and 300 kPa, using water as working fluid. Fig. 3b shows a photograph of the atomization pattern obtained using one of those nozzles. This and other purposely performed long exposure pictures indicated that the atomization angle for distances from the injector tip less than 205 mm does not change substantially and it is an average of 60 degrees for the wide range of the nozzle Reynolds number used in this study. This constant value is used instead of the slightly changing angle specified by the manufacturer as nominal, indicated in Table 3. The atomization of the solution was observed through the peepholes, checking that in all experiments the solution was fully atomized in small drops at the end of the absorbing spray. The disintegration of the liquid sheet in drops is beneficial because fresh liquid is exposed to vapour, as a result of the motion involved in atomization, improving the absorption rate. The height selected to locate the nozzle is 205 mm, measured from the bottom of the chamber.

3. Data reduction

3.1. Heat transfer analysis

In order to analyse the heat transfer in the subcooler, the experimental global heat transfer coefficients were determined in the FPHE using single-phase flows along both sides, thanks to a set of experiments developed using ammonia/lithium nitrate solution-

water combination as working fluids at each side of the heat exchanger. The coefficient was calculated as described in Zacarías [15]:

$$U_{\text{exp}} = \frac{q}{Fc \cdot \Delta T_{lm}} \quad (1)$$

The heat flux is:

$$q = \dot{Q} / A \quad (2)$$

where A is the effective heat transfer area of the FPHE and \dot{Q} is the thermal power exchanged:

$$\dot{Q} = \dot{m} \cdot (h_i - h_o) \quad (3)$$

The factor Fc in Eq. (1) is the correction factor of the logarithmic mean temperature difference ΔT_{lm} . This factor takes into account that the external plates of the subcooler transfer heat by only one side. Values of Fc have been taken from Shah and Kandlikar [27]. The logarithmic mean temperature difference is calculated from Eq. (4):

$$\Delta T_{lm} = \frac{\Delta T_1 - \Delta T_2}{\ln\left(\frac{\Delta T_1}{\Delta T_2}\right)} \quad (4)$$

where ΔT_1 and ΔT_2 are:

$$\Delta T_1 = T_{cs,i} - T_{w,o} ; \Delta T_2 = T_{cs,o} - T_{w,i} \quad (5)$$

3.2. Mass transfer analysis

The parameters described in this section allow evaluating the transfer of mass in the adiabatic absorber in alternative ways. Variables used in the definitions are determined as follows:

- The refrigerant mass fraction of the solution diluted by the refrigerant at the outlet of the absorber was determined by means of the correlation given by Libotean [26], of the form:

$$X_{ds} = f(T_{ds}, \rho_{ds}) \quad (6)$$

where the density ρ_{ds} and the temperature T_{ds} were experimentally measured.

- The refrigerant mass fraction of the concentrated solution at the inlet of the absorber was determined according to the following mass rate balance:

$$X_{cs} = \frac{X_{ds} \cdot \dot{m}_{ds} - \dot{m}_v}{\dot{m}_{cs}} \quad (7)$$

where the diluted solution mass flow rate \dot{m}_{ds} and the vapour mass flow rate \dot{m}_v were experimentally measured.

- The concentrated solution mass flow rate \dot{m}_{cs} was determined by means of the mass rate balance in the absorber:

$$\dot{m}_{cs} = \dot{m}_{ds} - \dot{m}_v \quad (8)$$

3.2.1. Absorption ratio

The absorption ratio R_a indicates how much vapour is being absorbed by each kilogram of solution circulated [9,11,12]. It is useful for cycle evaluation, as it is the inverse of the circulation ratio for single pass absorbers:

$$R_a = \frac{\dot{m}_v}{\dot{m}_{ds}} \quad (9)$$

3.2.2. Mass transfer coefficient

In the present paper the mass transfer coefficient is defined similarly to Kim *et al.* [28] and Miller and Keyhani [29] (in both cases falling film diabatic absorbers) and Palacios *et al.* [11] (adiabatic absorber). It indicates the mass conductance of the process.

$$h_m = \frac{G_v}{\rho_{ds} \cdot \Delta X_{lm}} \quad (10)$$

where:

$$G_v = \frac{\dot{m}_v}{A_a} \quad (11)$$

The reference area for mass transfer A_a has been defined in the literature in different ways, taking into account the absorption method used and the data available from the experiment. For example, Lee *et al.* [30] defined it as the plate absorber surface by which the multiphase flow was circulating, in that case a bubble absorber. Vallès *et al.* [31] used the area of the multiphase heat exchanger located downstream of the adiabatic absorption chamber. Arzoz *et al.* [8] defined A_a as the contact surface between liquid and vapour for the three cases under study, all of them of the adiabatic absorption type: falling film, continuous liquid jet and droplets of 4 mm diameter. Palacios *et al.* [12],

using flat fan nozzles and adiabatic absorption, added the interface of the liquid sheet to the overall interface area of the droplets generated during disintegration. Both magnitudes were estimated from flow visualization.

In the present paper, the area A_a used to calculate the mass transfer coefficient was defined as the surface area of the two flat solution sheets, as shown in figures 3a) and 3b). The total area of one sheet has been considered equal to two times (two sheet faces) the area of an isosceles triangle of 60° aperture angle and 205 mm height. This approach does not take into account the active surface area change of the ligaments and drops formed after fragmentation of the liquid sheet. However, it is a sensible choice for calculating and comparing the mass transfer coefficient. Besides this, it allows a direct use of the experimental results and indicates the envelope of the area occupied.

The logarithmic mean concentration difference ΔX_{lm} can be defined in different ways, as shown by Venegas *et al.* [7]. In the present study, it follows Palacios *et al.* [11,12] and Acosta-Iborra *et al.* [13]:

$$\Delta X_{lm} = \frac{\Delta X_1 - \Delta X_2}{\ln\left(\frac{\Delta X_1}{\Delta X_2}\right)} \quad (12)$$

$$\Delta X_1 = X_{eq,i} - X_{cs} \quad (13)$$

$$\Delta X_2 = X_{eq,o} - X_{ds} \quad (14)$$

In these equations, the saturation concentrations $X_{eq,i}$ and $X_{eq,o}$ are calculated using the absorber pressure and the local solution temperatures.

3.2.3. Outlet subcooling

The outlet subcooling $\Delta T_o \geq 0$ indicates how far the solution is from saturation at the absorber outlet, being null at equilibrium. It allows a direct evaluation of absorption performance when measuring outlet temperature.

$$\Delta T_o = T_{eq,a} - T_{ds} \quad (15)$$

The adiabatic equilibrium temperature $T_{eq,a}$ is determined following the procedure described in Section 3.2.5.

3.2.4. Approach to equilibrium factor

The approach to equilibrium factor F is a non-dimensional measure of the saturation grade that the solution has reached at the end of the absorption process. It allows direct comparison with numerical models.

$$F = \frac{X_{ds} - X_{cs}}{X_{eq,a} - X_{cs}} \quad (16)$$

The adiabatic equilibrium concentration $X_{eq,a}$ is also determined following the procedure described in section 3.2.5.

3.2.5. Equilibrium conditions for adiabatic absorption

The simultaneous resolution of the following equations allows determining the equilibrium conditions reached at the outlet of an adiabatic absorber:

Energy and global mass rate balance:

$$\dot{m}_{cs} \cdot h_{cs} + \dot{m}_{v,eq} \cdot h_v = (\dot{m}_{cs} + \dot{m}_{v,eq}) \cdot h_{eq,a} \quad (17)$$

Mass rate balance for the refrigerant:

$$\dot{m}_{cs} \cdot X_{cs} + \dot{m}_{v,eq} = (\dot{m}_{cs} + \dot{m}_{v,eq}) \cdot X_{eq,a} \quad (18)$$

The following equations relate the refrigerant mass fraction $X_{eq,a}$, temperature $T_{eq,a}$, pressure P_{eq} , and equilibrium enthalpy $h_{eq,a}$, for the solution used as working fluid:

$$P_{eq} = f(X_{eq,a}, T_{eq,a}); h_{eq,a} = f(X_{eq,a}, T_{eq,a}) \quad (19)$$

where the equilibrium pressure is the absorption one:

$$P_{eq} = P_a \quad (20)$$

For the inlet enthalpy, neglecting kinetic energy:

$$h_{cs} = f(X_{cs}, T_{cs}); h_v = f(P_a, T_v) \quad (21)$$

$T_{eq,a}$, $X_{eq,a}$, and $\dot{m}_{v,eq} / \dot{m}_{cs}$ are obtained as part of the solution of this system of equations. They are a function of X_{cs} , P_a , T_v and T_{cs} . A sensitivity analysis shows that T_v has a small influence within reasonable values, owing to the small value of $\dot{m}_{v,eq} / \dot{m}_{cs}$. Because of this, inlet conditions will be assumed at the same temperature T_{cs} from now on.

4. Results and discussion

4.1. Heat transfer in the subcooler

54 experiments in steady-state conditions were performed to thermally characterise the solution subcooler working under single-phase conditions. Table 4 gives the range of the operating parameters used in the experimental campaign: temperature of the solution at the inlet T_i , and outlet T_o , cooling water temperature at the inlet T_{wi} , and outlet T_{wo} , and mass flow rates of the solution \dot{m}_{cs} , and water \dot{m}_w .

Fig. 4 shows the experimental global heat transfer coefficients obtained using Eq. (1) for the plate subcooler as a function of the solution Reynolds number, evaluated at the inlet temperature. In spite of the low Reynolds number, heat transfer coefficients are between 113 and 525 W/m²K. These values are above those reported by Infante Ferreira [33], using also the ammonia-lithium nitrate solution, but in a diabatic vertical tubular absorber configuration based on bubbles. The higher values obtained here are attributed to the more favourable heat transfer, taking place now between single phase flows (liquid) at both sides of the heat exchanger, and the corrugations of the plate subcooler enhancing turbulence and heat transfer coefficients. This, jointly with the high compact construction, is one of the advantages of the separation of the mass and heat transfer processes in adiabatic absorbers.

4.2. Absorption using flat fan nozzles

In the analysis of the absorber, 14 experiments were recorded using the flat fan nozzles, controlling the solution subcooling (the inlet solution temperature, 24.5 – 29.7 °C) and the diluted solution mass flow rate (0.04 – 0.08 kg/s). The resulting vapour mass flow rate was between 0.7 – 2.5 g/s and the absorption pressure between 308 – 399 kPa. These two last variables are dependent on the controlled variables, as shown in Figs. 5 and 7. The opening of the vapour expansion valve was kept constant in these experiments, allowing pressure variations within the absorption chamber.

Increasing subcooling entails a higher capacity for vapour absorption inside the absorption chamber, allowing higher refrigerant mass fraction changes for a fixed solution mass flow rate. Thus, higher subcooling results in higher vapour mass flow

rate. Consequently, vapour separated in the generator increases, as the whole facility is working under steady state conditions and the absorber is the limiting component to increase capacity. Fig. 5 allows observing the experimentally obtained relation between vapour mass flow rate and inlet subcooling, $\Delta T_i = T_{eq,i} - T_{cs}$.

For a fixed inlet subcooling, the increase of the solution mass flow rate also implied a higher vapour mass flow rate, as can be observed in Fig. 5. When the solution mass flow rate augments, the fluid velocity increases and the smaller droplets are generated at a shorter distance from the injector tip. This interpretation was experimentally verified in the test rig. Consequently, more quantity of subcooled solution surface is available to absorb refrigerant vapour, overcoming the shorter residence time effect. The net result is an increase of the vapour mass flow rate.

On the other hand, in the present study experiments showed that, as the vapour mass flow rate augmented due to an increased subcooling, all the vapour entering to the absorption chamber was not fully absorbed, increasing pressure. Fig. 6 shows the approach to equilibrium factor for the different inlet subcooling experimented. As observed, this factor is not much affected by the solution subcooling. Fig. 7 depicts the relation between the absorption pressure and the two controlled variables, solution subcooling and mass flow rate. It can be seen that higher subcooling is proportionally related to higher absorption pressures.

The influence of the controlled variables (inlet subcooling and solution mass flow rate) on the absorption ratio, mass transfer coefficient, outlet subcooling and approach to equilibrium factor is shown in the following.

The absorption ratio R_a as a function of the inlet subcooling is shown in Fig. 8. As it can be expected, absorption is promoted by subcooling. Lower inlet solution temperature increases the separation of the solution from its equilibrium state at the absorption pressure, increasing the ammonia mass flux to the solution. Duplication of the subcooling implies also duplication of the absorption ratio. This linear correlation coincides with findings reported by Arzo *et al.* [8] and Palacios *et al.* [12].

Absorption ratios found in this work are similar to those theorized by Acosta-Iborra *et al.* [13], although only a qualitative comparison is possible as in that work a steady sheet was considered with no atomization. They are higher than those obtained by Palacios *et al.* [12] using a similar nozzle. In their study, when locating the spray approximately 205 mm above the bottom of the absorption chamber, they reached

absorption ratios in the range 5.5-10 g/kg (in the present study between 15.8 and 29.6 g/kg). The difference between both experimental results could be attributed to:

- Differences in the inlet subcooling of both solutions. 10 °C and 15 °C were used by Palacios *et al.* [12], while in the present study it was varied between 11.7 °C and 23.8 °C.
- Differences in the thermal and transport properties between the working solutions. Palacios *et al.* [12] used water-lithium bromide, while in the present study ammonia-lithium nitrate was employed.
- Differences between dimensions of the flat fan-sheet and droplets size generated in each case. The much lower vapour density for water-lithium bromide reduces the liquid sheet instabilities and reduces the residence time because of the lower aerodynamic drag.

Another figure of merit than can be used to characterise the adiabatic absorber is the outlet subcooling, defined in section 3.2.3. Fig. 9 represents this variable as a function of the Reynolds number Re_a . As it can be observed, outlet subcooling is small and decreases as the nozzle Reynolds number increases. It could be attributed to the higher instabilities in the flat fan-sheet and the smaller diameters of the resulting droplets, inducing higher inter-phase surface and consequently higher mass transfer rates. The high values of the metrological uncertainties show that outlet subcooling is not an accurate variable to evaluate the performance of the adiabatic absorber, as it is shown in the Fig. 9 error bars.

In spite of this difficulty, one can say that the outlet subcoolings found in this paper are lower than those reported by Summerer *et al.* [5] using binary and ternary hydroxide mixtures (NaOH, KOH and CsOH) and water as refrigerant. These authors used fog jet, full jet and spiral nozzles. When the atomizer was located 200 mm above the liquid surface, the smallest outlet subcooling was 1.9 °C. The better results here obtained can be attributed also to reasons similar to those commented before, when comparing with results of Palacios *et al.* [12], besides a different spray geometry.

Fig. 10 shows the approach to equilibrium factor F (defined in Eq. (16)) for three different inlet solution mass flow rates as a function of the nozzle Reynolds number Re_a . Results indicate the increase of F when Re_a increases. As this figure shows, high values of F have been obtained.

Just as a qualitative reference, the values of F obtained in this work are slightly higher and respectively higher than the falling film and continuous jet, both essayed by Arzoz *et al.* [8] in an adiabatic absorber. In that work, the authors used the water-lithium bromide solution. However the present results for F are similar to those obtained by Palacios *et al.* [12] using also the water-lithium bromide and a flat fan-sheet in an adiabatic absorber.

The influence of the Reynolds number over the outlet subcooling and F , in Fig. 9 and 10 respectively, can be evaluated by means of the statistical significance of the slope using a linear fit [34]. The uncertainty of the data is included in the linear fit obtained. This approach has been used in the present study using EESTM [21], obtaining a ratio between the slope and its standard deviation equal to 3.6 and 4.7 respectively. Based on these results, it can be concluded that the decrease in the outlet subcooling and increase in F , obtained when Reynolds number increases, is statistically significant.

Fig. 11 shows the relation between the mass transfer coefficient h_m and the nozzle Reynolds number Re_a . Both variables show a direct linear relation, again supporting the enhanced absorption effect with increasing Re_a . Table 5 shows a comparison between values of h_m obtained in different studies. It can be observed that adiabatic absorbers allow obtaining high mass transfer coefficients.

4.3. Mass transfer correlations

The approach to equilibrium factor F is a useful parameter for the absorber design of absorption refrigeration systems and does not need an arbitrary reference area. Zacarías [15] showed that this parameter much influenced the results of a numerically modelled thermo-chemical compressor using it as input. As far as the authors' knowledge, Warnakulasuriya and Worek [9] obtained the only experimental correlation available for F , in this case as a function of the Sherwood number Sh . They used the highly viscous fluid LZBTM supplied by the company TraneTM.

With the aim of obtaining a useful correlation for the design of adiabatic absorbers, in the present study a dimensional analysis was developed. The variables relevant to F were identified, namely: inlet solution mass flow rate \dot{m}_{cs} , vapour mass flow rate \dot{m}_v , inlet solution temperature T_{cs} , inlet subcooling ΔT_i , outlet solution equilibrium temperature $T_{eq,a}$, absorption heat ΔH , inlet solution pressure P_{cs} , absorber pressure P_a ,

refrigerant mass fraction of the inlet solution X_{cs} , density ρ_v, ρ_{cs} , and viscosity μ_{cs}, μ_{cs} , of both vapour and inlet solution, and specific heat Cp_{cs} , thermal conductivity k_{cs} , surface tension σ_{cs} , and diffusion coefficient D_{cs} , of the inlet solution:

$$f(\dot{m}_{cs}, \dot{m}_v, T_{cs}, T_{eq,a}, \Delta H, a, P_{cs}, P_a, X_{cs}, \rho_v, \rho_{cs}, \mu_v, \mu_{cs}, Cp_{cs}, k_{cs}, \sigma_{cs}, D_{cs}, d_o) = 0 \quad (22)$$

Using the theorem Pi of Buckingham and by means of a statistical analysis using multiple linear regressions, a correlation for F using dimensionless groups has been obtained. Most influential non-dimensional groups have been identified through a sensitivity analysis within the tested ranges. The best correlation obtained, with the goodness of fit parameter $R^2 = 76.6\%$, is:

$$F = 114.63 Re_a^{0.064} Le^{-3.319} Pr^{3.293} \quad (23)$$

with: $1,401 < Re_a < 3,404$; $292.9 < Le < 346.3$; $59.7 < Pr < 70.2$

The Sherwood number is an alternative figure of merit, useful to characterise mass transfer processes:

$$Sh = \frac{h_m \cdot L^*}{D_{cs}} \quad (24)$$

where L^* is the characteristic length, equal to 0.205 m, here defined as the height of the absorption spray.

Under isothermal absorption, theory of mass transfer by forced convection predicts that the Sherwood number is correlated with Reynolds and Schmidt numbers, Welty *et al.* [36]:

$$Sh = C_1 \cdot Re_a^{C_2} Sc^{C_3} \quad (25)$$

where C_1, C_2 and C_3 are constants obtained experimentally.

In the present study, the following correlation was obtained with $R^2 = 99.1\%$:

$$Sh = 0.763 \cdot Re_a^{1.329} Sc^{0.936} \quad (26a)$$

with:

$$1,401 < Re_a < 3,404 \quad ; \quad 17,472 < Sc < 24,304 \quad (26b)$$

Eq. (26a) indicates a negligible effect of absorption heating on these experiments.

The solution temperature at the absorption chamber inlet has been used to calculate all properties in Eqs. (23) to (26).

Fig. 12 and 13 show a comparison between experimental and predicted values of the approach to equilibrium factor F and Sherwood number Sh using Eqs. (23) and (26)

respectively. All of the predicted data differ less than 2.6% and 7.7% respectively from the experimental data, offering good correlations.

These equations can be of profit for the simulation and design of adiabatic absorbers using flat-fan atomizers and the ammonia-lithium nitrate solution in the operating conditions defined by the ranges of the dimensionless groups, typical for a single effect chiller.

Table 6 offers results of the maximum uncertainty obtained for main variables calculated in the present study.

5. Conclusions

From the analysis of the heat and mass-transfer taking place respectively in the subcooler and adiabatic chamber, considered as components of an adiabatic absorber, the following conclusions can be derived:

Referring to the heat transfer process in the subcooler:

- Taking into account that the Reynolds numbers are low, global heat transfer coefficients obtained in the plate heat exchanger using the ammonia-lithium nitrate solution can be considered favourable. They are approximately two times higher than the results available from a vertical tubular bubble absorber. Owing to the high compactness of plate heat exchangers, this supports the potential of the adiabatic absorber concept.

Referring to the mass transfer process in the adiabatic absorption chamber:

- Inlet solution subcooling is a variable having a clear positive effect over the absorption ratio. However, in the present experiments it was observed that the approach to equilibrium factor is not much affected by the inlet solution subcooling.
- The approach to equilibrium factors obtained in the present study are high and comparable to those from previously published results. This allows designing absorption chambers of about 200 mm height. These results indicate that the use of flat fan nozzles is positive to improve absorption in adiabatic absorbers and of value for $\text{NH}_3\text{-LiNO}_3$ solution.

- Correlations for the approach to equilibrium factor and Sherwood number have been obtained. They can be used to anticipate the performance of adiabatic absorbers.

Acknowledgements

The financial support of this study by the Spanish Ministry of Education and Science research grant ENE2005-08255-C02-02, ENE2009-11097 and Project CCG07-UC3M/ENE-3411, by the Local Government of Madrid and UC3M, is greatly appreciated. A. Zacarías also acknowledges the financial support given by National Board of Science and Technology and the Instituto Politécnico Nacional of Mexico. The authors want to acknowledge the help of Mr. Manuel Santos and Mr. Carlos Cobos in the laboratory work.

References

- [1] K.E. Herold, R. Radermacher, S. Klein, Absorption chillers and heat pumps, CRC Press, New York, 1996.
- [2] C.A. Infante Ferreira, Vertical tubular absorbers for ammonia-salt absorption refrigeration, Ph.D. Thesis, Delft Technical University, Delft, Holland, 1985.
- [3] W.A. Ryan, Water absorption in an adiabatic spray of aqueous lithium bromide solution, in: AES-Vol. 31, International Absorption heat Pump Conference, ASME, 1993, pp. 155-162.
- [4] W.A. Ryan, F. Ruiz, J. Wurm, Model development and verification of spray absorption for gas driven cooling systems, in: Proceedings of International Gas Research Conference, Cannes, 1995, pp. 1483-1493.
- [5] F. Summerer, F. Ziegler, P. Riesch, G. Alefeld, Hydroxide absorption heat pumps with spray absorber, ASHRAE Technical Data Bulletin 12 (1996) 50-57.
- [6] M. Venegas, M. Izquierdo, P. Rodríguez, A. Lecuona, Heat and mass transfer during absorption of ammonia vapour by $\text{LiNO}_3\text{-NH}_3$ solution droplets, Int. J. Heat Mass Transf. 47 (2004) 2653–2667.

- [7] M. Venegas, P. Rodríguez, A. Lecuona, M. Izquierdo, Spray absorbers in absorption systems using lithium nitrate–ammonia solution, *Int. J. Refrig.* 28 (2005) 554–564.
- [8] D. Arzoz, P. Rodríguez, M. Izquierdo, Experimental study on the adiabatic absorption of water vapor into LiBr-H₂O Solutions, *Appl. Therm. Eng.* 25 (2005) 797-811.
- [9] F.S.K. Warnakulasuriya, W.M. Worek, Adiabatic water absorption properties of an aqueous absorbent at very low pressures in a spray absorber, *Int. J. Heat Mass Transf.* 49 (2006) 1592-1602.
- [10] F.S.K. Warnakulasuriya, W.M. Worek, Drop formation of swirl-jet nozzles with high viscous solution in vacuum-new absorbent in spray absorption refrigeration, *Int. J. Heat Mass Transf.* 51 (2008) 3362-3368.
- [11] E. Palacios, M. Izquierdo, R. Lizarte, J.D. Marcos, Lithium bromide absorption machines: pressure drop and mass transfer in solutions conical sheets, *Energy Conv. Manag.* 50 (2009) 1802-1809.
- [12] E. Palacios, M. Izquierdo, J.D. Marcos, R. Lizarte, Evaluation of mass absorption in LiBr flat-fan sheets, *Appl. Energy* 86 (2009) 2574-2582.
- [13] A. Acosta-Iborra, N. García, D. Santana, Modelling non-isothermal absorption of vapour into expanding liquid sheets, *Int. J. Heat Mass Transf.* 52 (2009) 3042-3054.
- [14] G. Gutiérrez, Thermo-fluid dynamic evaluation of components in adiabatic absorption systems, Ph.D. Thesis, Universidad Carlos III de Madrid, Spain, 2009.
- [15] A. Zacarías, Transferencia de masa y calor en absorbedores adiabáticos con aplicación de la disolución nitrato de litio-amoniaco, Ph.D. Thesis, Universidad Carlos III de Madrid, Spain, 2009.
- [16] R. Ventas, Estudio de máquinas de absorción con la disolución nitrato de litio-amoniaco. Ciclos híbridos potenciados con compresión mecánica, Ph.D. Thesis, Universidad Carlos III de Madrid, Spain, 2010.
- [17] S. Jeong, S. Garimella, Falling-film and droplet mode heat and mass transfer in a horizontal tube LiBr/water absorber, *Int. J. Heat Mass Transf.* 45 (2002) 1445-1458.

- [18] M. Venegas, M. Izquierdo, M. de Vega, A. Lecuona, Thermodynamic study of multistage absorption cycles using low-temperature heat, *Int. J. Energy Res.* 26 (2002) 775-791.
- [19] A. Zacarías, R. Ventas, M. Venegas, A. Lecuona, Boiling heat transfer and pressure drop of ammonia-lithium nitrate solution in a plate generator, *Int. J. Heat Mass Transf.* 53 (2010) 4768-4779.
- [20] R. Ventas, A. Lecuona, M. Legrand, M.C. Rodriguez-Hidalgo, On the recirculation of ammonia-lithium nitrate in adiabatic absorber for chillers, *Appl. Therm. Eng.* 39 (2010) 2770-2777.
- [21] S.A. Klein, Engineering Equation Solver. Versión Académica-profesional, 1992-2008, V8.186-3D, 2008.
- [22] R. Tillner-Roth, F. Harms-Watzenberg, H.D. Baehr, Eine neue Fundamentalgleichung für Ammoniak, *DKV-Tagungsbericht* 20 (1993) 167-181.
- [23] L. Haar, J.S. Gallagher, G.S. Kell, NBS/NRC Steam Tables, Hemisphere Publishing Co., 1984.
- [24] S. Libotean, D. Salavera, M. Vallés, X. Esteve, A. Coronas, Vapor-liquid equilibrium of ammonia+lithium nitrate+water and ammonia+lithium nitrate solutions from (293.15 to 353.15) K, *J. Chem. Eng. Data* 52 (2007) 1050-1055.
- [25] S. Libotean, A. Martín, D. Salavera, M. Vallés, X. Esteve, A. Coronas, Densities, viscosities and heat capacities of ammonia-lithium nitrate and ammonia-lithium nitrate-water solutions between (293.15 and 353.15) K, *J. Chem. Eng. Data* 53 (2008) 2383-2388.
- [26] S.N. Libotean, Caracterización termofísica de la mezcla ternaria amoniac/nitrato de litio/agua para aplicaciones de refrigeración por absorción, Ph.D. Thesis, Universitat Rovira i Virgili, Spain, 2008.
- [27] R.K. Shah, S.G. Kandlikar, The influence of the number of thermal plates on heat exchanger performance, Hemisphere Publishing Corp., pp. 267-288, 1986.
- [28] J.K. Kim, N.S. Bernan, D.S.C. Chau, B.D. Wood, Absorption of water vapour into falling films of aqueous lithium bromide, *Int. J. Refrig.* 18 (1995) 486-495.
- [29] W.A. Miller, M. Keyhani, The correlation of simultaneous heat and mass transfer experimental data for aqueous lithium bromide vertical falling film absorption, *J. Sol. Energy Eng. Trans. -ASME* 123 (2001) 30-42.

- [30] K.B. Lee, B.H. Chun, J.C. Lee, C.H. Lee, S.H. Kim, Experimental analysis of bubble mode in a plate-type absorber, *Chem. Eng. Sci.* 57 (2002) 1923-1929.
- [31] M. Vallès, M. Bourouis, D. Boer, A. Coronas, Absorption of organic fluid mixtures in plate heat exchanger, *Int. J. Therm. Sci.* 42 (2003) 85-94.
- [32] F.P. Incropera, D.P. De-Witt, *Fundamentos de Transferencia de Calor*, 4th edition, Pearson Prentice Hall, Mexico, 1999.
- [33] C.A. Infante Ferreira, Operating characteristics of $\text{NH}_3\text{-LiNO}_3$ and $\text{NH}_3\text{-NaSCN}$ absorption refrigeration machines, in: 19th International Congress of Refrigeration, Vol. IIIa, 1995, pp. 321-328.
- [34] C. Salter, Error analysis using the variance-covariance matrix, *J. Chem. Educ.* 77 (2000) 1239-1243.
- [35] J. Cerezo, M. Bourouis, M. Vallès, A. Coronas, R. Best, Experimental study of an ammonia–water bubble absorber using a plate heat exchanger for absorption refrigeration machines, *Appl. Therm. Eng.* 29 (2009) 1005-1011.
- [36] J.R. Welty, C.E. Wicks, R.E. Wilson, *Fundamentals of momentum, heat and mass transfer*, John Wiley & Sons Inc., pp. 929, 2001.

Fig. 1. Layout of the experimental setup.

Fig. 2. Scheme of the FPHE used as solution subcooler.

Fig. 3a. Scheme of the adiabatic absorber. **Fig. 3b.** Photograph of the atomization pattern of the injector in Table 3, corresponding to a solution pressure drop equal to 140 kPa and an injection height of 205 mm. Indicates a 60 deg. atomization angle.

Fig. 4. Global heat transfer coefficient in the subcooler and comparison with data from [33]. The uncertainties of the global heat transfer coefficient are shown.

Fig. 5. Vapour mass flow rate as a function of the inlet subcooling for three different inlet solution mass flow rates.

Fig. 6. Approach to equilibrium factor as a function of the solution inlet subcooling. The uncertainties of the approach to equilibrium factor are shown.

Fig. 7. Absorption pressure as a function of the inlet subcooling for three different inlet solution mass flow rates.

Fig. 8. Relation between absorption ratio and inlet subcooling. The uncertainties of the absorption ratio are shown.

Fig. 9. Relation between outlet subcooling and nozzle Reynolds number for three values of the solution mass flow rate. The uncertainties of the outlet subcooling are shown.

Fig. 10. Approach to equilibrium factor as a function of the nozzle Reynolds number for three inlet solution mass flow rates. The uncertainties of the approach to equilibrium factor are shown.

Fig. 11. Mass transfer coefficient as a function of the nozzle Reynolds number. The uncertainties of the mass transfer coefficient are shown.

Fig. 12. Correlated vs. experimental F .

Fig. 13. Correlated vs. experimental Sh .

Highlights of paper ATE-2010-1173

Adiabatic absorption of NH_3 vapour into $\text{NH}_3\text{-LiNO}_3$ using flat fan nozzle created spray

A linear relation exists between solution inlet subcooling and absorption ratio

The approach to equilibrium factor is always between 0.81 and 0.89 at 205 mm height

Experimental values of mass transfer coefficient and outlet subcooling are presented

Correlations for the approach to equilibrium factor and the Sherwood number are given

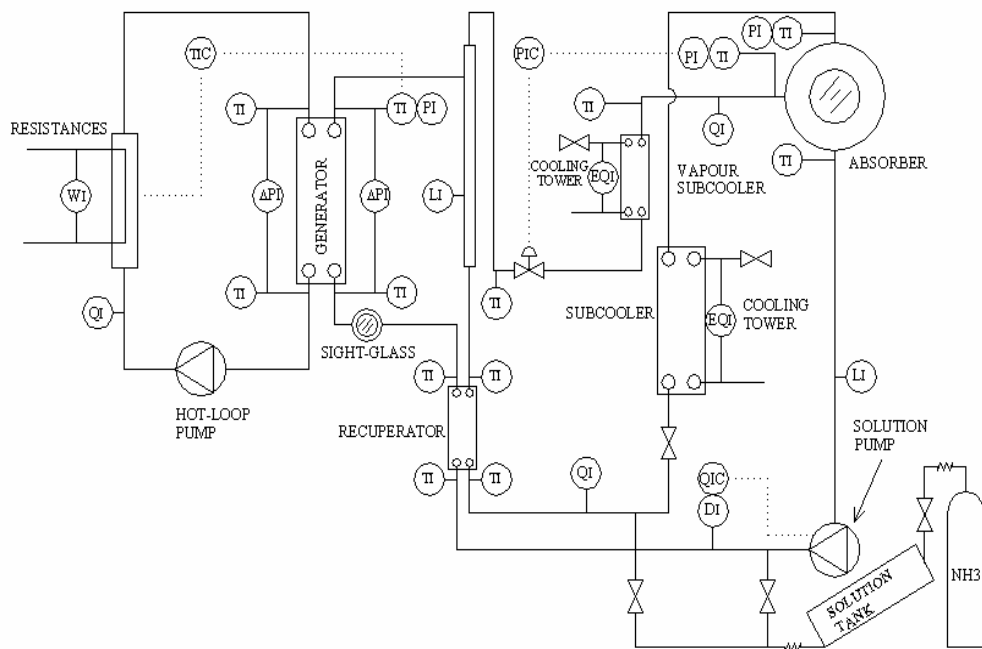


Fig. 1. Layout of the experimental setup.

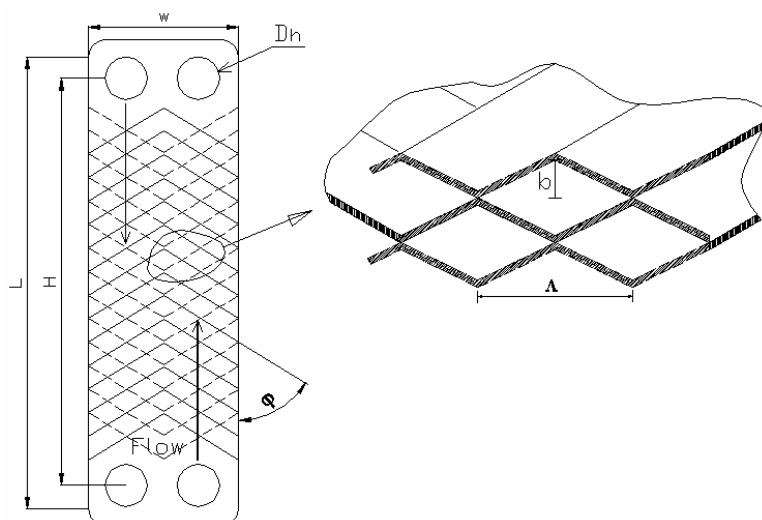
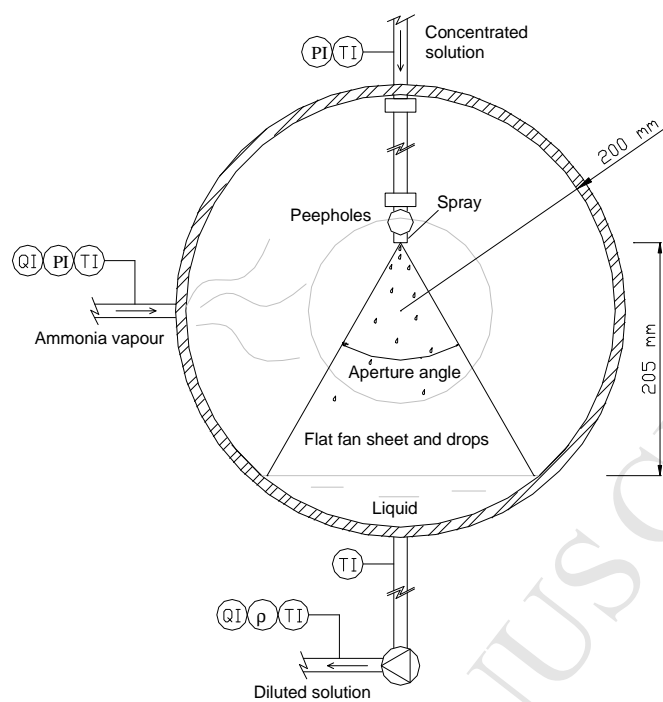


Fig. 2. Scheme of the FPHE used as solution subcooler.



a)



b)

Fig. 3a. Scheme of the adiabatic absorber. **Fig. 3b.** Photograph of the atomization pattern of the injector in Table 3, corresponding to a solution pressure drop equal to 140 kPa and an injection height of 205 mm. Indicates a 60 deg. atomization angle.

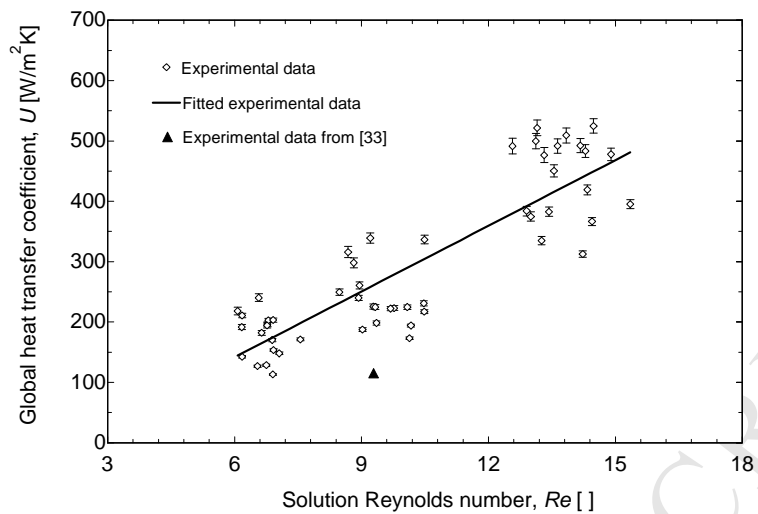


Fig. 4. Global heat transfer coefficient in the subcooler and comparison with data from [33]. The uncertainties of the global heat transfer coefficient are shown.

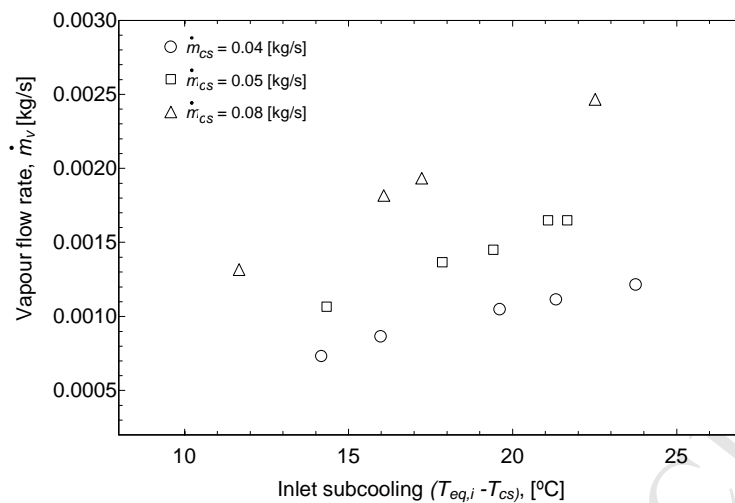


Fig. 5. Vapour mass flow rate as a function of the inlet subcooling for three different inlet solution mass flow rates.

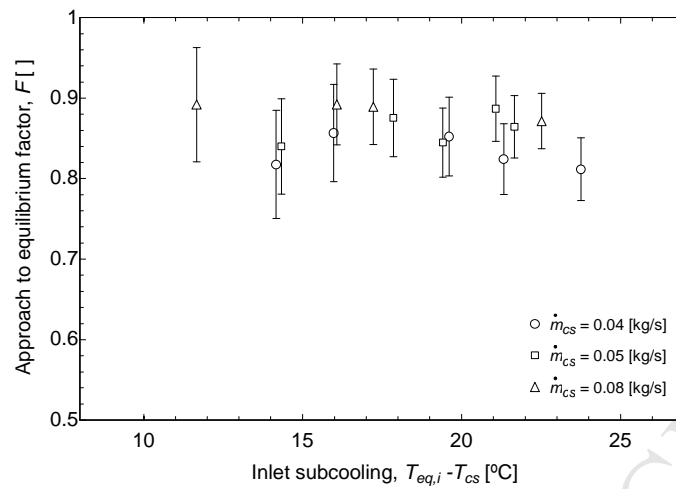


Fig. 6. Approach to equilibrium factor as a function of the solution inlet subcooling. The uncertainties of the approach to equilibrium factor are shown.

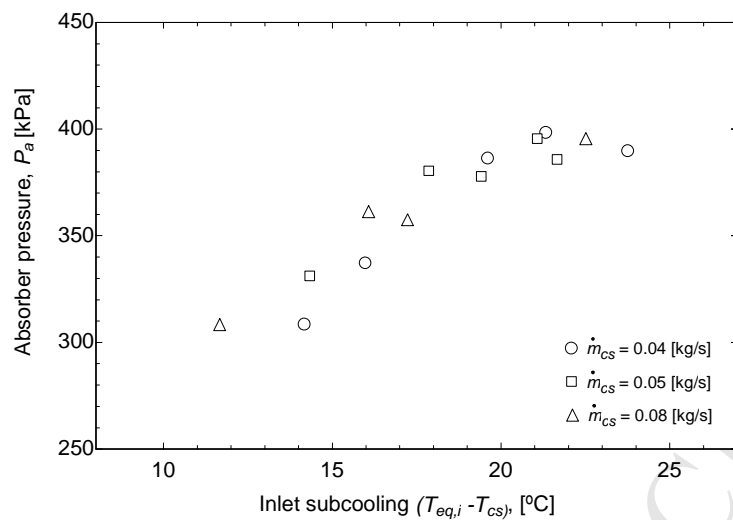


Fig. 7. Absorption pressure as a function of the inlet subcooling for three different inlet solution mass flow rates.

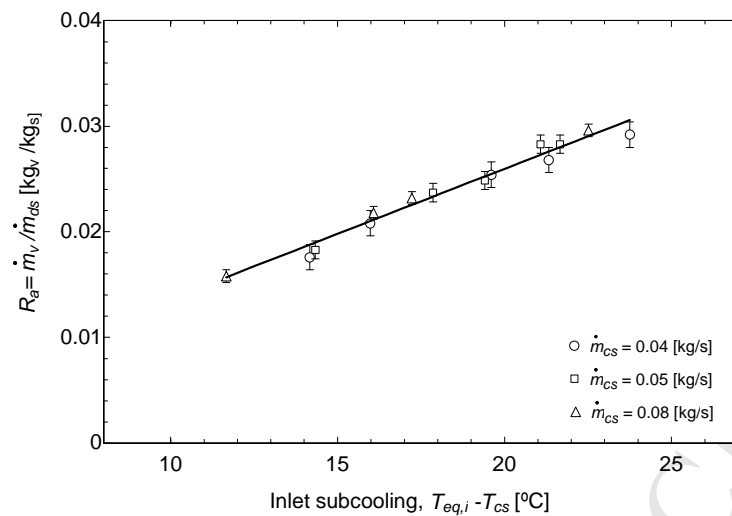


Fig. 8. Relation between absorption ratio and inlet subcooling. The uncertainties of the absorption ratio are shown.

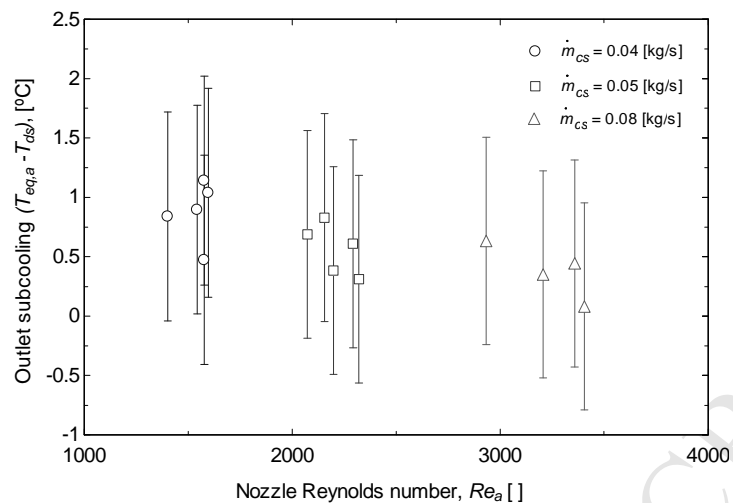


Fig. 9. Relation between outlet subcooling and nozzle Reynolds number for three values of the solution mass flow rate. The uncertainties of the outlet subcooling are shown.

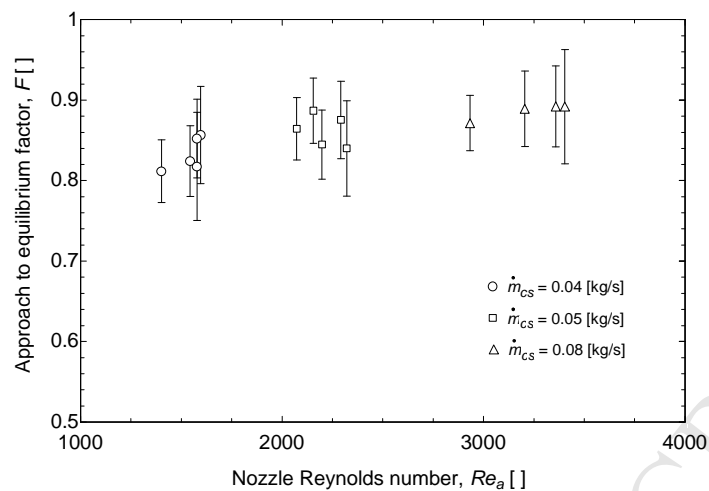


Fig. 10. Approach to equilibrium factor as a function of the nozzle Reynolds number for three inlet solution mass flow rates. The uncertainties of the approach to equilibrium factor are shown.

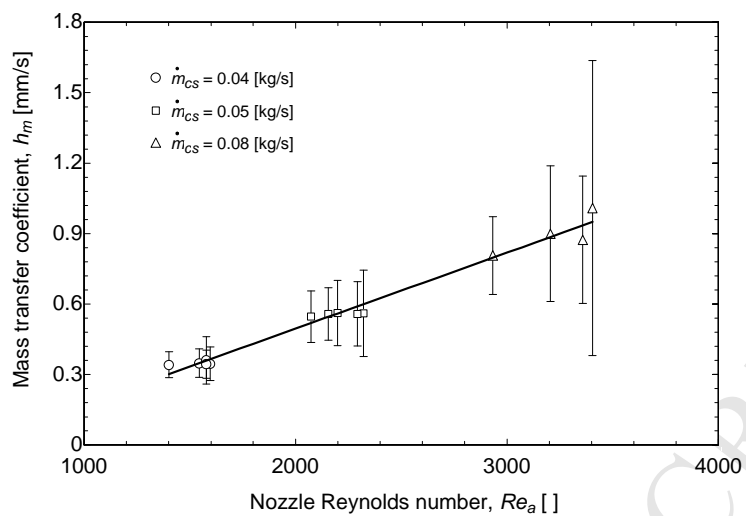


Fig. 11. Mass transfer coefficient as a function of the nozzle Reynolds number. The uncertainties of the mass transfer coefficient are shown.

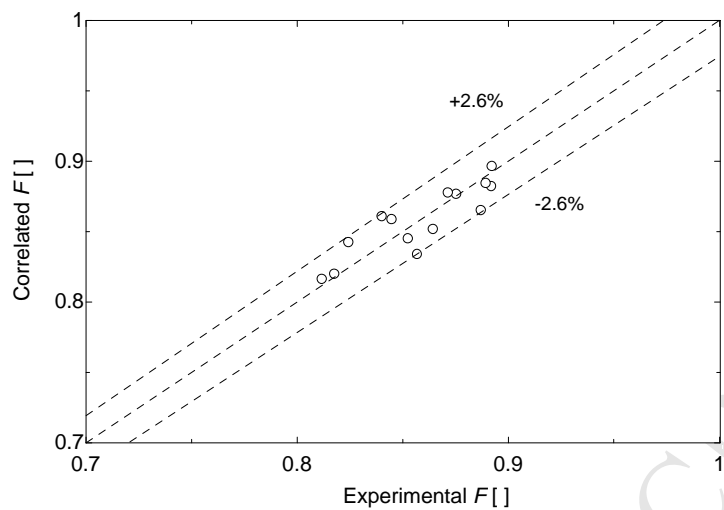


Fig. 12. Correlated vs. experimental F .

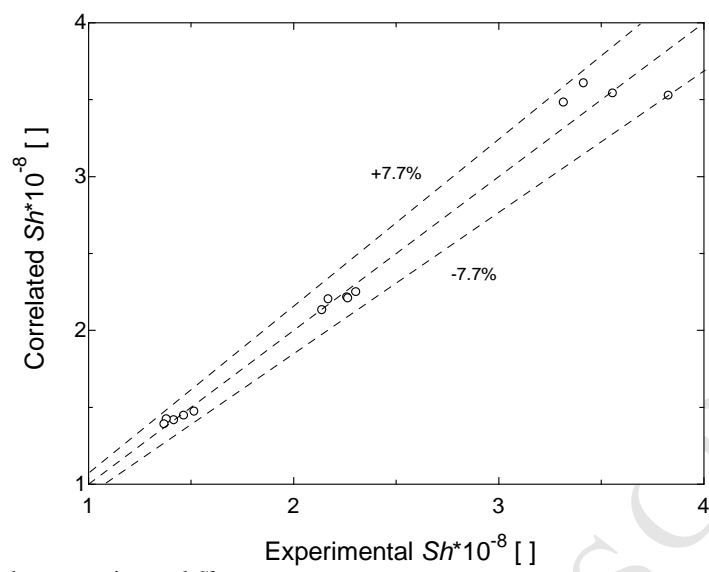


Fig. 13. Correlated vs. experimental Sh .

Table 1

Results of the uncertainty analysis for measured variables.

Variable	Type	Range	Uncertainty
T of the solution at the absorber inlet/subcooler outlet	Thermoresistance PT100	10-60 °C	±0.40 °C
T of the solution at the absorber outlet	Thermoresistance PT100	10-60 °C	±0.58 °C
T of the solution at the subcooler inlet	Thermoresistance PT100	10-110 °C	±0.39 °C
T of the vapour at the absorber inlet	Thermoresistance PT100	10-60 °C	±0.51 °C
T of the water at the subcooler inlet	Thermoresistance PT100	10-50 °C	±0.24 °C
T of the water at the subcooler outlet	Thermoresistance PT100	10-50 °C	±0.21 °C
P at the absorber inlet	Absolute pressure transducer	0-1 MPa	±1 kPa
P_a	Absolute pressure transducer	0-1 MPa	±1 kPa
\dot{m}_{ds}	Coriolis flow meter	0-0.3 kg/s	±0.03% f.s.
\dot{m}_w	Microflow meter	0-3.47 kg/s	±0.2%
ρ_{ds}	Coriolis flow meter	0-10,000 kg/m ³	±0.03% f.s.
\dot{m}_v	Coriolis flow meter	0-0.1 kg/s	±0.05% f.s.

Table 2

Geometrical parameters of the FPHE used as solution subcooler. Model AN76 of Alfa Laval™. See Fig. 2 for further details.

Parameter	Value
Number of plates (N)	20
Heat transfer effective area of the plate (A)	0.1 m ²
Surface enlargement factor (ϕ)	1.22
Channel height (b)	2.4 mm
Hydraulic diameter (D_h)	3.9 mm
Channel width (w)	175 mm
Effective thermal length (L)	576 mm
Vertical distance between port centers (H)	519 mm
Port diameter (D_p)	54 mm
Plate thickness (e)	0.4 mm
Corrugation pitch (Λ)	9.85 mm
Corrugations angle (ϕ)	58.5 degrees

Table 3

Nozzle specifications from Spraying Systems Co™.

Model	¼ H-VV SS 65 06	
Equivalent hole diameter (d_o)	1.5 mm	
Pressure drop	150 kPa	300 kPa
Atomization angle	54 deg	65 deg
Capacity	1.7 l/min	2.4 l/min

Table 4

Range of the operating parameters used to characterize the solution subcooler.

Variable	Parameter	Range
T_i	Solution temperature at the inlet of the subcooler	50-70 °C
T_o	Solution temperature at the outlet of the subcooler	24-30 °C
$T_{w,i}$	Inlet cooling water temperature	9-19 °C
$T_{w,o}$	Outlet cooling water temperature	36-56 °C
\dot{m}_{cs}	Solution mass flow rate	0.04; 0.06; 0.08 kg/s
\dot{m}_w	Water mass flow rate	0.05-0.13 kg/s

Table 5

Comparison between mass transfer coefficients h_m reported in the literature.

Reference	Absorber type	Configuration	Method	Solution	$h_m \cdot 10^5$ (m s ⁻¹)
Vallès <i>et al.</i> [31]	Diabatic in PHE	Spray (full cone)	Experimental	Organic mixtures	1 – 2.5
Cerezo <i>et al.</i> [35]	Diabatic	Bubble	Experimental	NH ₃ -H ₂ O	100 – 200
Venegas <i>et al.</i> [7]	Adiabatic	Spray (full cone)	Numerical	NH ₃ -LiNO ₃	8.1 – 86
Arzoz <i>et al.</i> [8]	Adiabatic	Falling film	Experimental	H ₂ O-LiBr	1 – 15
Palacios <i>et al.</i> [12]	Adiabatic	Spray (flat fan)	Experimental	H ₂ O-LiBr	30
This work	Adiabatic	Spray (flat fan)	Experimental	NH ₃ -LiNO ₃	34 – 101

Table 6

Results of the uncertainty analysis for the calculated variables with a confidence level of 95%.

Variable	Type	Uncertainty
Global heat transfer coefficient, U	Relative	$\pm 22.2\%$
Absorption ratio, R_a	Relative	$\pm 7.1\%$
Inlet subcooling, ΔT_i	Absolute	± 0.97 °C
Outlet subcooling, ΔT_o	Absolute	± 0.88 °C
Approach to equilibrium factor, F	Relative	$\pm 8.3\%$
Mass transfer coefficient, h_m	Relative	$\pm 62.3\%$